

Ultra High Speed LiNbO₃ and Polymer Electrooptic Modulators in Lightwave Optical Access Communication Networks

Dr. Ahmed Nabih Zaki Rashed

*Electronics and Electrical Communications Engineering Department
Faculty of Electronic Engineering, Menouf 32951, Menoufia University, EGYPT
ahmed_733@yahoo.com*

Abstract

In the present paper, we have been modeled parametrically and numerically the high speed of materials based electrooptic (EO) modulators in advanced optical communication systems. The modulated bandwidth is deeply and parametrically studied over wide ranges of the affecting sets of parameters via specially designed software which processes the interaction of causes and effects. The design parameters of the lumped circuit have been processed over large operating requirements. Lithium niobate (LiNbO₃) external modulators can also offer pure phase modulation in coherent systems and can realize various optical signal processors. As the bit rate of optical network systems becomes higher, it becomes more difficult to drive a modulator with a high voltage. Therefore, reduction of the driving voltage of an LiNbO₃ modulator with a broadband characteristic is an extremely important issue for realizing future high speed optical transmission systems. Moreover polymer electrooptic devices have been extensively studied and explored due to its intrinsic advantages over conventional materials such as high speed operation, compatibility with other materials and substrates.

Keywords: *Electrooptic devices, electrooptic modulation, optical polymers, Lithium niobate, slab and rib waveguides.*

1. Introduction

Present communication technology relies on fiber optic systems which include light sources such as a laser, optical fiber, integrated optical components such as modulators and switches, and optical detectors. The lasers and detectors are fabricated using semiconductor materials, and the integrated optical components are generally fabricated using electrooptic single crystal materials such as lithium niobate (LiNbO₃). Among the integrated optical components, the contribution from electrooptic modulators using LiNbO₃ waveguide structures has been significant in the last several decades due to their high-speed [1]. The essential requirements for efficient electrooptic modulation are low half-wave (switching) voltage and broad 3-dB modulation bandwidth. High-speed traveling-wave electro optic modulators are very important devices because of their applications in many optoelectronic fields, such as telecommunication, optical signal processing, and optical measurement. With the increasing demand for broadband communication, many studies on the high-speed electro optic modulators have been carried out for optical communication system [2]. In addition, the precise control of the frequency responses of high-speed electro optic modulators has been required for the new generation optical fiber communication systems. In a standard traveling-wave electrooptic modulator, the frequency response of the modulation index is restricted by

two effects: the velocity mismatching between the lightwave and modulation microwave and the loss of modulation microwave in the traveling-wave electrodes [3].

Electrooptic modulators have a number of telecommunication and scientific applications, including analog optical links, optical signal processing (OSP), and frequency comb generation [4]. These types of modulators have an enhanced modulation response within a finite bandwidth of typically a few gigahertz around resonance. Ring resonators made from EO polymer materials have certain advantages over other material choices such as LiNbO_3 , most notably the low microwave/optical velocity mismatch allowing for simple design of high-speed modulation devices. For instance, demonstrations driving an EO polymer Mach-Zehnder (MZ) modulator beyond 100 GHz have been reported previously [5]. In addition, the photolithographic fabrication capabilities of EO polymer enable easy integration of complex OSP structures [6].

In the present study, LiNbO_3 , and Polymer electrooptic external modulators have been developed for extensive use in high speed and long distance optical fiber transmission systems. This is because they can offer the advantages of modulation exceeding multi Gbit/sec combined with a low driving voltage, and they can eliminate the dynamic laser wavelength chirping which limits the span-rate system product due to their fiber dispersion characteristics.

2. Types of Modulation Schemes

It is well known that the electrical signal still conquers our communication terminals in everyday life. But to take advantage of the optical transmission system, these electrical signals must be converted into optical ones which can be transferred in fibers. The electrooptic modulator as shown in Fig. 1, is such a device that converts the electrical signal to the optical one and passed it to the amplification process stage.

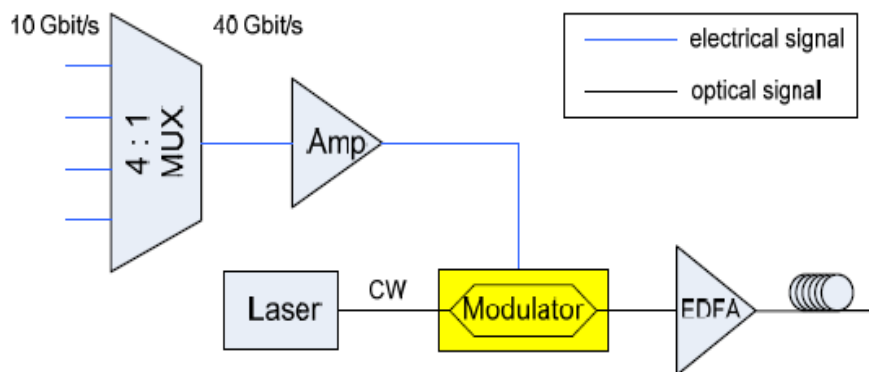


Fig. 1. Electrooptic Modulator Function in the Transmitter System.

In addition, high bandwidth optical modulation has also applications in fiber optic radio frequency signal transmission and optoelectronic signal processing [7].

2. 1. Direct Modulation Scheme

The most straightforward method for modulation is to directly modulate the laser source. Due to the requirements of bandwidth and efficiency, only semiconductor lasers are of practical interest for direct modulation. A unique feature of semiconductor lasers is that the

semiconductor laser can be modulated directly by modulating the excitation current. As shown in Fig. 2, for a semiconductor laser, the output power of light intensity increases linearly with the injection current above threshold.

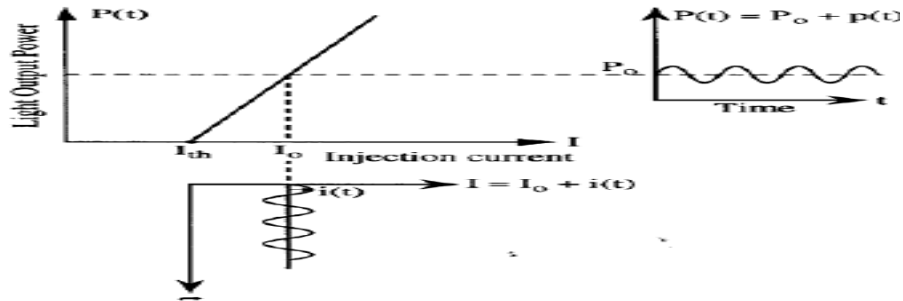


Fig. 2. Transition function of a current modulated semiconductor laser

For an injection current $I = I_0 + i(t)$, the optical output power is $P(t) = P_0 + p(t)$, where (I_0, P_0) is the bias point for the direct modulation of the semiconductor laser [8]. Using this feature, the direct modulation scheme can be configured as shown in Fig. 3.

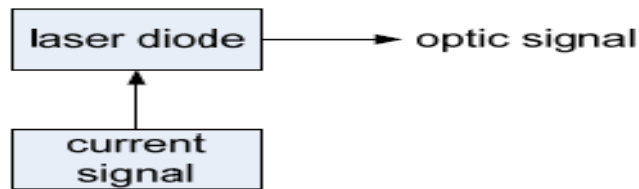


Fig. 3. Direct Modulation Scheme

However, when the modulation frequency increases toward the relaxation resonance frequency of a semiconductor laser, both the relative intensity noise and distortions increase rapidly [8]. This severely limits the feasibility of direct modulation for a higher frequency. The large frequency chirp also precludes the direct modulation for long-distance communications systems.

2. 2. External Modulation Scheme

At bit rates of 10 Gbit/s or higher, the frequency chirp imposed by direct modulation becomes large enough that direct modulation of semiconductor laser is rarely used [9]. Unlike direct modulation, external modulation has been shown to have superior performance for wide bandwidth optical fiber communications, however with the potential disadvantages of adding system complexity and cost.

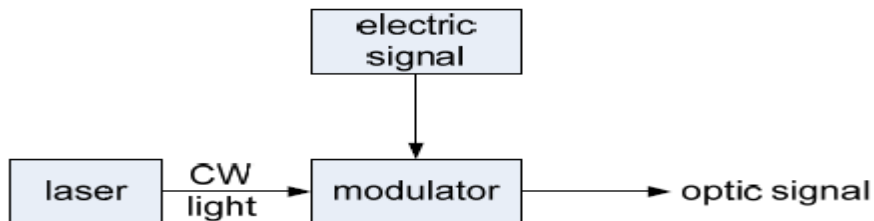


Fig. 4. External Modulation Scheme

As shown in Fig. 4, for a high-speed transmitter, the laser is biased at a constant current to provide the continuous wave (CW) output, and an external optical modulator placed next to the laser converts the CW light into a data coded pulse train with correct modulation format. In the external modulation scheme, the light output passes through a material whose optical properties can be modified by an applied external electric field. External optical modulators with bandwidths greater than 10 GHz are typically fabricated from the electro-optic crystal LiNbO_3 , electro-optic polymers or III-V semiconductor compounds. Some of these devices have shown modulation frequencies in excess of 40 GHz [10].

3. Lumped Element Circuit Model

At frequencies where the wavelength is several orders of magnitude larger than the greatest dimensions of the circuit or system being examined, conventional circuit elements such as capacitors, inductors and resistors are the basic building blocks for the circuits or systems. The description or analysis of such circuits may be adequately carried out in terms of loop currents and node voltages without consideration of propagation effects.

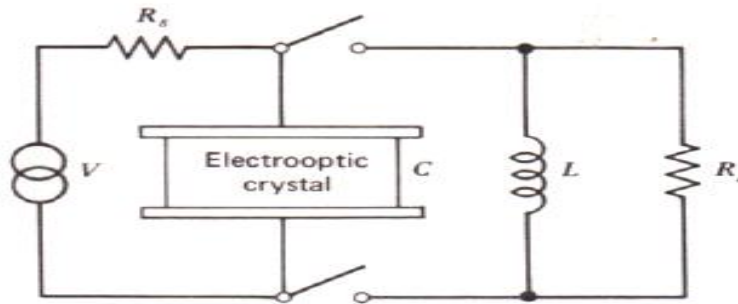


Fig. 5. Equivalent circuit of an electrooptic modulator

However, as the frequency is raised to a point where the wavelength is no longer large compared to the circuit dimensions, propagation effects can no longer be ignored [10]. As shown in Fig. 2, the maximum modulation bandwidth (the frequency spectrum occupied by the modulation signal) must be less than (with $R_L=R_S$).

4. Theoretical Model Analysis

Both the input power P_i and the output power P_o of the modulator are given by [11]:

$$P_m = \frac{V_m^2}{2R_L}, \text{ Watt} \quad (1)$$

$$P_0 = \frac{\Gamma_m^2 \lambda^2 A \varepsilon \Delta \nu}{4\pi L_m n_0^6 r_{33}^2}, \text{ Watt} \quad (2)$$

Where V_m is the modulating voltage, R_L is the load resistance, Γ_m is the peak retardation of the modulating voltage, $\varepsilon = \varepsilon_0 \cdot \varepsilon_r$ is the dielectric constant at the modulation frequency ω_0 , A is the cross-section area, $\Delta \nu$ is the modulation bandwidth, L_m is the modulator length, n_0 is the refractive index of the material, r_{33} is the elect-optic coefficient. The resonance frequency ω_r and the angular bandwidth $\Delta \omega$ can be expressed as the following:

$$\omega_r^2 = \frac{1}{LC} - \frac{L^2}{r^2}, \quad (3)$$

$$\Delta\omega = \frac{1}{RC} \quad (4)$$

Where r is the linear ratio of ON power to OFF power, R is the resistance of the lumped circuit, C is the capacitance of the lumped circuit. Also we have in the electrooptic modulators, the peak retardation of modulation voltage is given by the following formula:

$$\Gamma_m = \frac{\pi V_m}{V_\pi} \quad (5)$$

Where V_π is the voltage required to change the output light intensity from its maximum value to its minimum value or modulator half wave voltage can be expressed as [11].

$$V_\pi = \frac{\lambda}{2n_0^3 r_{33}} \quad (6)$$

Assuming that cross section under the square configuration that $A = L_m^2$, the modulator efficiency is given by:

$$\eta = \frac{P_{in}}{P_0} = L_m \varepsilon \Delta\omega R n_0^6 \quad (7)$$

$$\text{and } \frac{\eta C}{L_m} = \varepsilon_0 n_0^6 \quad (8)$$

Thus η is proportional to modulator length L_m and inversely proportional to capacitance of lumped circuit C . Therefore to design at maximum efficiency i.e., $\eta = 1$, we must make the condition:

$$C = L_m \cdot \varepsilon_0 \cdot n_0^6 \quad (9)$$

To work at certain modulation frequency ω_0 , we must make the condition:

$$L = \frac{1}{\omega_0^2 \cdot C} \quad (10)$$

To work at given angular bandwidth $\Delta\omega$, we must have:

$$R = \frac{1}{\Delta\omega \cdot C} \quad (11)$$

In the general case, if $\eta \ll 1$, the capacitance, inductance and resistance of modulator device, we have:

$$C = \frac{L_m \varepsilon_0 n_0^6}{\eta} \quad (12)$$

$$L = \frac{1}{\omega_0^2 C} = \frac{\eta}{\omega_0^2 L_m \varepsilon_0 n_0^6} \quad (13)$$

$$\text{and } R = \frac{1}{\Delta\omega C} \quad (14)$$

Then The 3-dB bandwidth of the electrooptic modulator device can be expressed as:

$$BW_{3-dB} = \frac{\Delta\omega}{2\pi} \quad (15)$$

4. 1. Materials Based Electrooptic Modulator

4. 1. 1. LiNbO₃ material

The investigation of both the thermal and spectral variations of the waveguide refractive index (n_0) require Sellmeier equation. The set of parameters required to completely characterize the temperature dependence of the refractive-index is given below, Sellmeier equation is under the form [12]:

$$n_0^2 = A_1 + A_2F + \frac{A_3 + A_4F}{\lambda^2 - (A_5 + A_6F)^2} + \frac{A_7 + A_8F}{\lambda^2 - A_9^2} - A_{10}\lambda, \quad (16)$$

Where λ is the optical signal wavelength in μm and $F = T^2 - T_0^2$, T is the ambient temperature in K, and T_0 is the room temperature and is considered as 300 K. The set of parameters of Sellmeier equation coefficients (LiNbO₃) are recast and dimensionally adjusted as below [12]: $A_1=5.35583$, $A_2=4.629 \times 10^{-7}$, $A_3=0.100473$, $A_4=3.862 \times 10^{-8}$, $A_5=0.20692$, $A_6=-0.89 \times 10^{-8}$, $A_7=100$, $A_8=2.657 \times 10^{-5}$, $A_9=11.34927$, and $A_{10}=0.01533$. Equation (16) can be simplified as the following:

$$n_0^2 = A_{12} + \frac{A_{34}}{\lambda^2 - A_{56}^2} + \frac{A_{78}}{\lambda^2 - A_9^2} - A_{10}\lambda, \quad (17)$$

Where: $A_{12}=A_1+A_2F$, $A_{34}=A_3+A_4F$, $A_{56}=A_5+A_6F$, and $A_{78}=A_7+A_8F$. Then the first and second differentiation of Eq. (16) with respect to operating wavelength λ which gives:

$$\frac{dn_0}{d\lambda} = \left(\frac{-\lambda}{n_0} \right) \cdot \left(\frac{A_{34}}{(\lambda^2 - A_{56}^2)^2} + \frac{A_{78}}{(\lambda^2 - A_9^2)^2} - A_{10} \right), \quad (18)$$

$$\frac{d^2n_0}{d\lambda^2} = \left(\frac{1}{n_0} \right) \cdot \left(\frac{A_{34}(2 - (\lambda^2 - A_{56}^2))}{(\lambda^2 - A_{56}^2)^3} + \frac{A_{78}(2 - (\lambda^2 - A_9^2))}{(\lambda^2 - A_9^2)^3} + A_{10} \right), \quad (19)$$

4. 1. 2. Polymer material

The refractive index of this material based electrooptic modulator can be [12]:

$$n_0 = \frac{B_1\lambda^2}{\lambda^2 - B_2^2} + \frac{B_3\lambda^2}{\lambda^2 - B_4^2} + \frac{B_5\lambda}{\lambda^2 - B_6^2} \quad (20)$$

The set of parameters of Sellmeier equation coefficients (PMMA) are recast below [12]: $B_1=0.4963$, $B_2=0.0718 (T/T_0)^2$, $B_3=0.6965$, $B_4=0.1174 (T/T_0)^2$, $B_5=0.3223$, and $B_6=9.237 (T/T_0)^2$. Where T is the ambient temperature, and T_0 is the room temperature. Then the first and second differentiation of Eq. (20) with respect to operating wavelength λ yields the following expressions:

$$\frac{dn_0}{d\lambda} = \frac{-1}{n_0} \left(\frac{B_1B_2^2\lambda}{(\lambda^2 - B_2^2)^2} + \frac{B_3B_4^2\lambda}{(\lambda^2 - B_4^2)^2} + \frac{B_5B_6^2}{(\lambda^2 - B_6^2)^2} \right), \quad (21)$$

$$\frac{d^2n_0}{d\lambda^2} = \frac{1}{n_0} \left(\frac{B_1B_2^2(3\lambda^2 + B_2^2)}{(\lambda^2 - B_2^2)^3} + \frac{B_3B_4^2(3\lambda^2 + B_4^2)}{(\lambda^2 - B_4^2)^3} + \frac{B_5B_6^2(3\lambda^2 - B_6^2)}{(\lambda^2 - B_6^2)^3} - \left(\frac{dn_0}{d\lambda} \right)^2 \right), \quad (22)$$

4. 1. 3. Transmission bit rate capacity

The total system rise time is the square root of the sum of the squares of the transmitter, optical fiber connection, and receiver rise times. That is given by [13]:

$$\tau_s = \sqrt{\tau_t^2 + \tau_{mat}^2 + \tau_r^2} , \quad (23)$$

The material dispersion time of the single mode fiber τ_{mat} , which is given by the following equation [14]:

$$\tau_{mat} = -\left(\frac{L_m \cdot \Delta\lambda \cdot \lambda}{c}\right) \cdot \left(\frac{d^2 n_0}{d\lambda^2}\right) , \quad (24)$$

In addition to providing sufficient power to the receiver, the system must also satisfy the bandwidth requirements imposed by the rate at which data are transmitted. A convenient method of accounting for the bandwidth is to combine the rise times of the various system components and compare the result with the rise time needed for the given data rate and pulse coding scheme. The system rise time is given in terms of the data rate for non return to zero pulse code by the expression [13, 14]:

$$B_R(NRZ) = \frac{0.7}{\tau_s} , \quad (25)$$

Then the bandwidth length product for electrooptic modulator device is given by [13, 14]:

$$P_R(NRZ) = B_R \cdot L_m , \text{ Gbit.cm/sec} \quad (26)$$

The bandwidth for single mode fibers for both materials based electrooptic modulator L_m is given by [13, 14]:

$$B.W_{sig.} = \frac{0.44}{\tau_s \cdot L_m} , \text{ GHz} \quad (27)$$

The signal to noise ratio (SNR) is a measure of signal quality at the receiver side, it is given by [15]:

$$SNR = \frac{(G P_0 \rho)^2 R_L}{4kT B.W_{sig.} + 2e R_L B.W_{sig.} G^n (I_D + \rho P_0)} , \quad (28)$$

$$(SNR)_{dB} = 10 \log SNR , \quad (29)$$

Where P_0 is the received or output optical power, ρ is the detector's unamplified responsivity, G is the detector gain if an avalanche photodiode (APD) is used, n accounts for the excess noise of the APD (usually between 2 and 3), $B.W_{sig.}$ is the signal bandwidth at the receiver, k is Boltzmann's constant ($k = 1.38 \times 10^{-23}$ J/K), e is the magnitude of the charge on an electron (1.6×10^{-19} coulomb), T is the ambient temperature in K, I_D is the detector's dark current, and R_L is the resistance of the load resistor that follows the photodetector. The maximum transmission bit rate or capacity according to modified Shannon technique is given by [16]:

$$B_R(SH) = B.W_{sig.} \log_2(1 + SNR) , \quad (30)$$

Where $B.W_{sig}$ is the actual bandwidth of the optical signal, and SNR is the signal to noise ratio in absolute value (i. e., not in dB). Where the Shannon bandwidth-length product can be given by [17, 18]:

$$P_{SH} = B_{R(SH)} \cdot L_m, \text{ Tbit.cm/sec} \quad (31)$$

5. Simulation Results and Performance Analysis

We have investigated ultra high speed LiNbO₃ and polymer electrooptic modulator devices in advanced optical communication systems over wide range of the affecting operating parameters as shown in Table 1.

Table 1: Proposed operating parameters for our suggested electrooptic modulator device.

Operating parameter	Definition	Value and unit
T	Ambient temperature	300 K ≤ T ≤ 340 K
L _m	Modulator length	2 cm ≤ L _m ≤ 5 cm
τ _t	Rise time of the transmitter	0.8 nsec
τ _r	Rise time of the receiver	1 nsec
P ₀	Output power	0.2 Watt ≤ P ₀ ≤ 0.597 Watt
T ₀	Room temperature	300 K
λ	Operating signal wavelength	0.4 μm ≤ λ ≤ 1.4 μm
Δλ	Spectral line width of the optical source	0.1 nm ≤ Δλ ≤ 0.3 nm
r ₃₃	Electrooptic coefficient for LiNbO ₃	31 Pm/volt
	Electrooptic coefficient for polymer	300 Pm/volt
L	Inductance	20 μH ≤ L ≤ 120 μH
C	Capacitance	0.2 pF ≤ C ≤ 2 pF
R _L	Load resistance	5 kΩ ≤ R _L ≤ 50 kΩ
G	Detector gain	20 dB ≤ G ≤ 50 dB
I _D	Detector dark current	8 nA
ρ	detector responsivity	0.25 A/Watt ≤ ρ ≤ 0.8 A/Watt
η	Modulator efficiency	60 % ≤ η ≤ 95 %
ε ₀	Dielectric permittivity	8.854 x10 ⁻¹⁴ F/cm
ε _r	Relative permittivity	2.5
c	Speed of light	3x10 ⁸ m/sec

Based on the model equations analysis, assumed set of the operating parameters, and the set of the Figs. (6-29), the following facts are assured as the following results:

- i) Figs. (6, 7) have demonstrated that as the optical signal wavelength increases for both LiNbO₃, and polymer materials increases, the refractive index of both materials decreases at constant ambient temperature. But as ambient temperature increases, refractive index of polymer material decreases at constant optical signal wavelength. Moreover as ambient temperature increases, refractive index of LiNbO₃ material increases at constant optical signal wavelength.

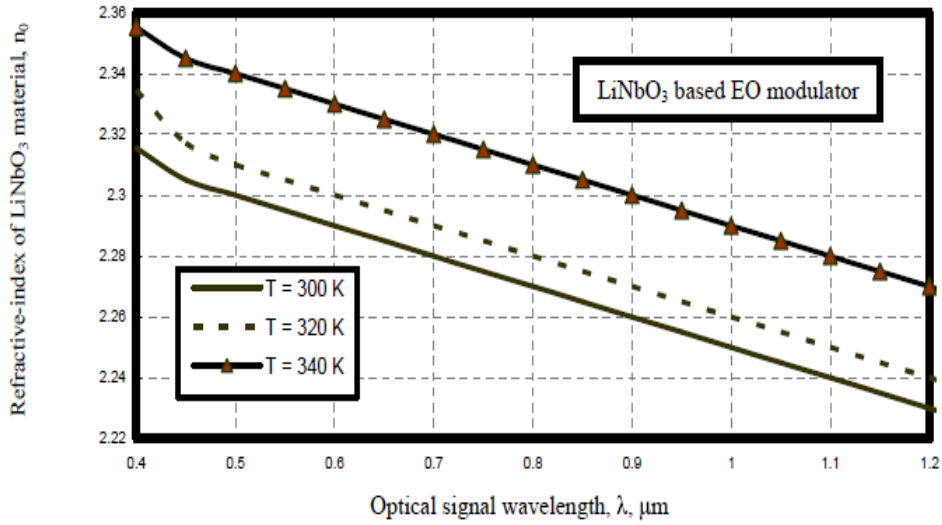


Fig. 6. Variations of refractive-index versus optical signal wavelength at the assumed set of parameters.

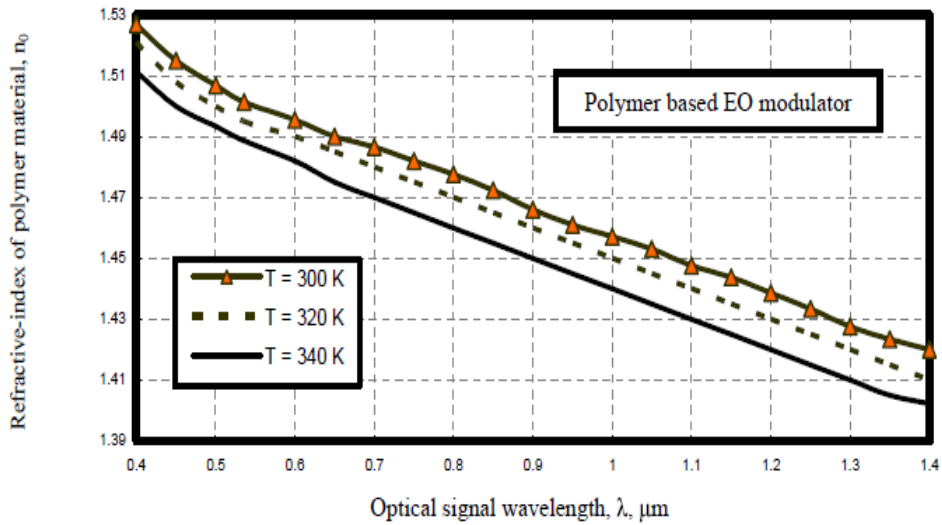


Fig. 7. Variations of refractive-index versus optical signal wavelength at the assumed set of parameters.

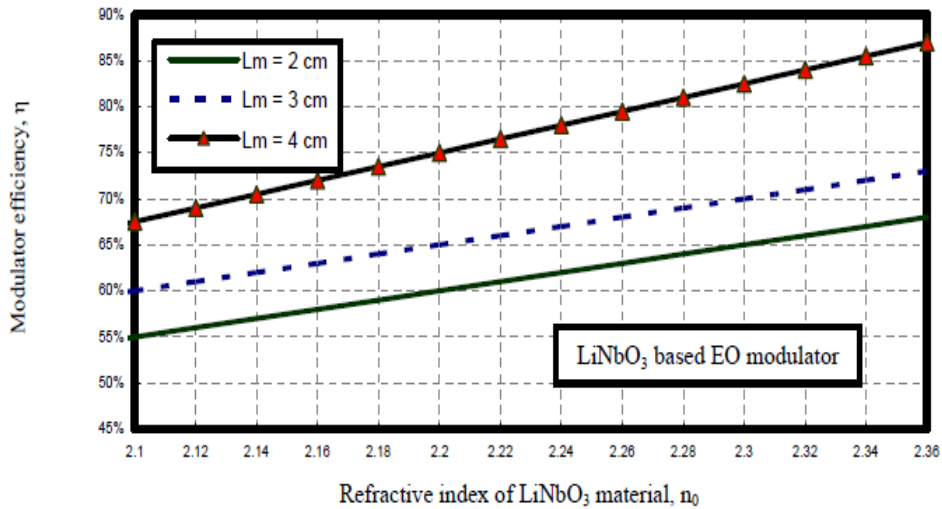


Fig. 8. Variations of modulator efficiency versus refractive index of LiNbO₃ at the assumed set of parameters.

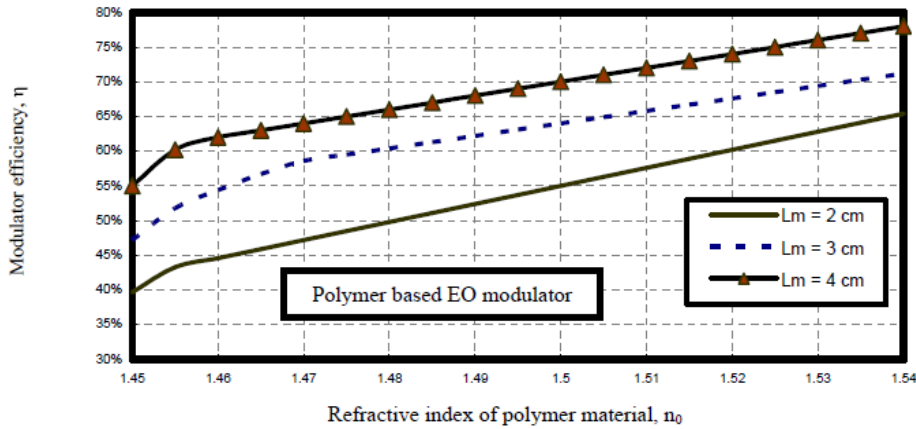


Fig. 9. Variations of modulator efficiency versus refractive index of polymer at the assumed set of parameters.

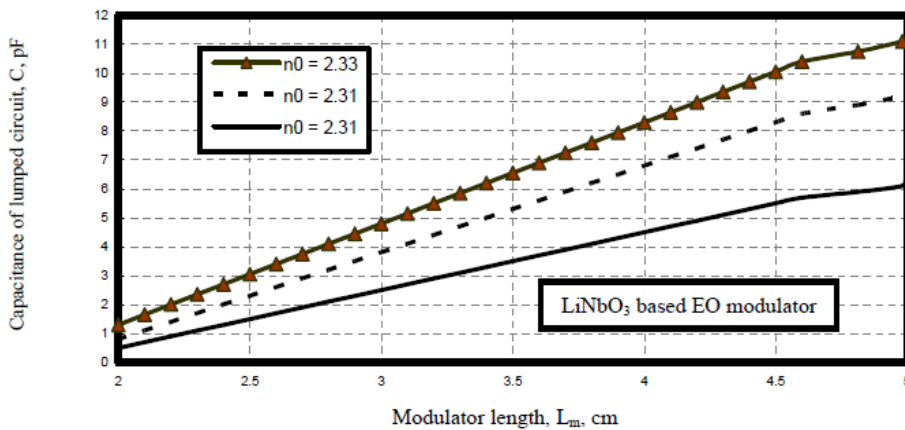


Fig. 10. Variations of capacitance of lumped circuit versus modulator length at the assumed set of parameters.

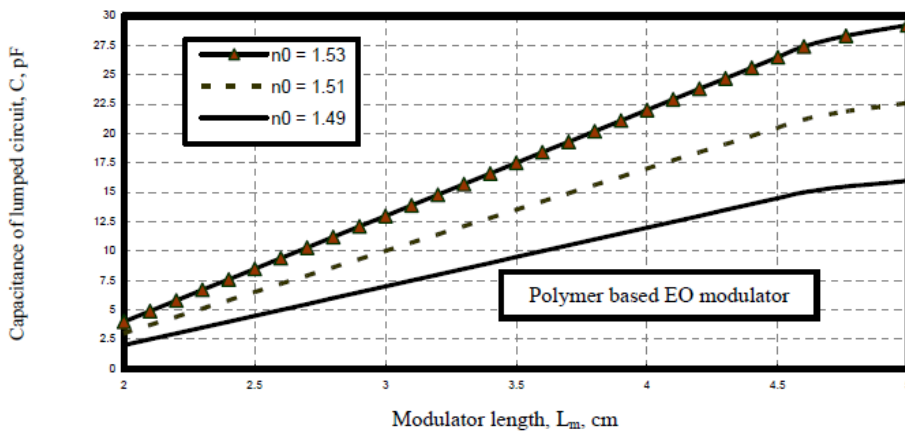


Fig. 11. Variations of capacitance of lumped circuit versus modulator length at the assumed set of parameters.

ii) As shown in the series of Figs. (8, 9), has proved that as refractive index of LiNbO_3 , and polymer materials increases, the modulator efficiency increases at constant modulator length. Moreover as modulator length based on these materials increases, the modulator length also increases.

iii) Figs. (10, 11) have assured that modulator length increases, capacitance of lumped circuit increases for both materials based EO modulator device at constant refractive

index. As well as refractive index increases for both materials based EO modulator device, capacitance of lumped circuit also increases at constant modulator length.

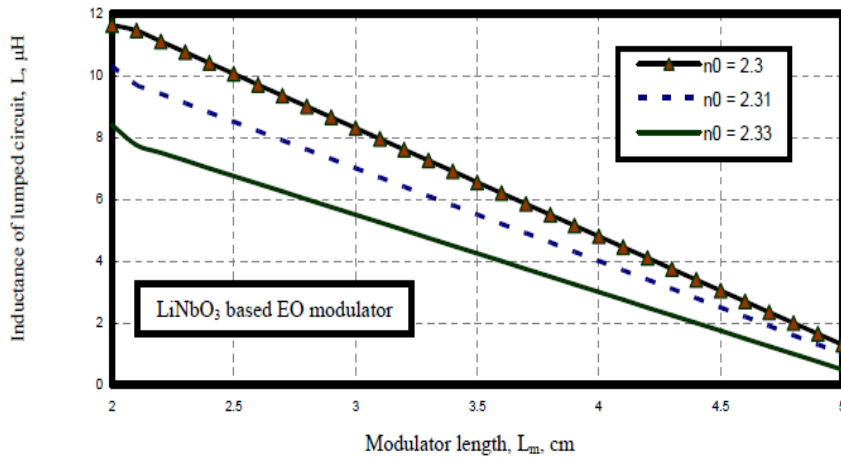


Fig. 12. Variations of inductance of lumped circuit versus modulator length at the assumed set of parameters.

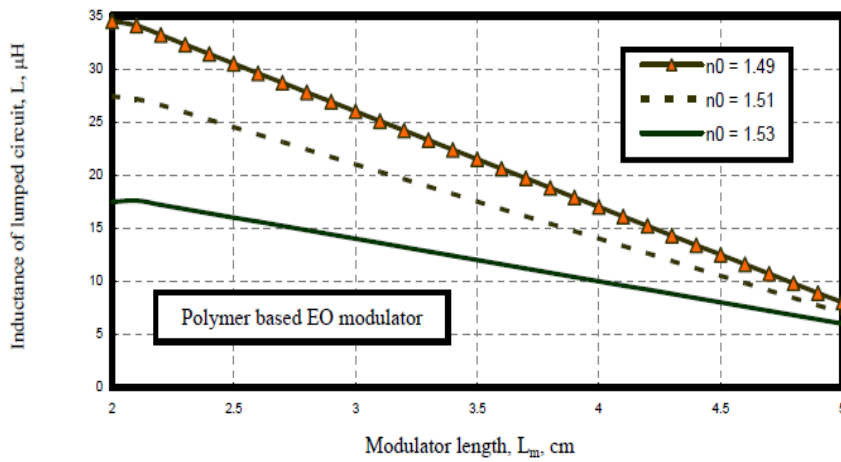


Fig. 13. Variations of inductance of lumped circuit versus modulator length at the assumed set of parameters.

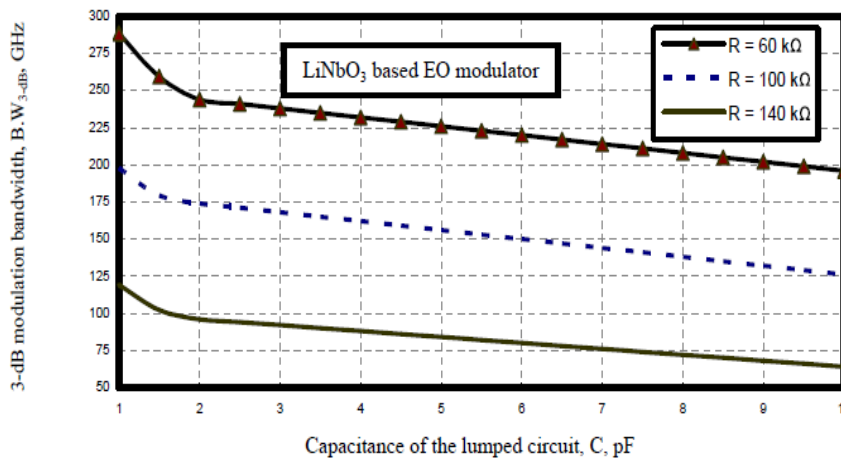


Fig. 14. Variations of 3-dB bandwidth versus capacitance of the lumped circuit at the assumed set of parameters.

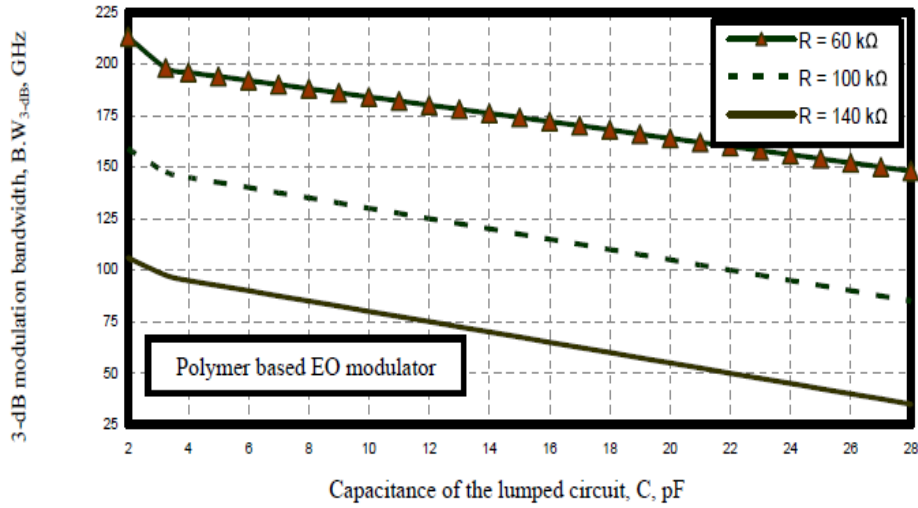


Fig. 15. Variations of 3-dB bandwidth versus capacitance of the lumped circuit at the assumed set of parameters.

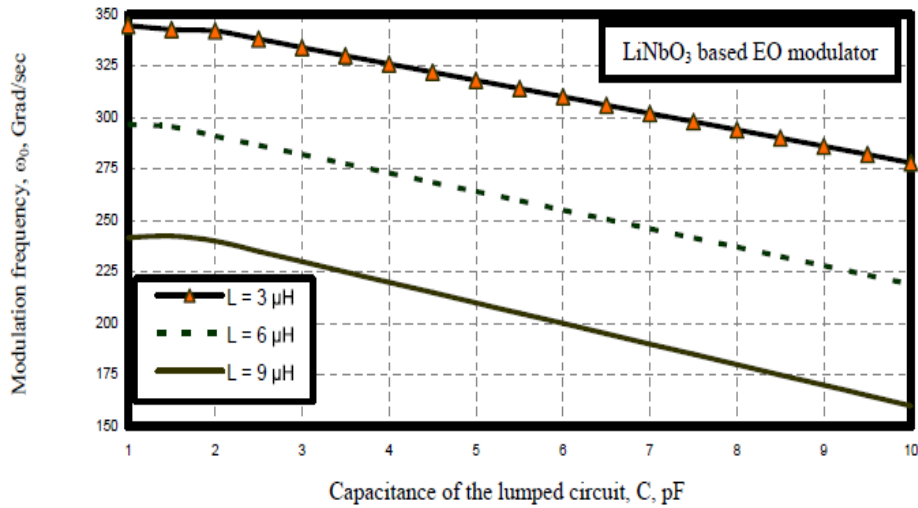


Fig. 16. Variations of modulation frequency versus capacitance of circuit at the assumed set of parameters.

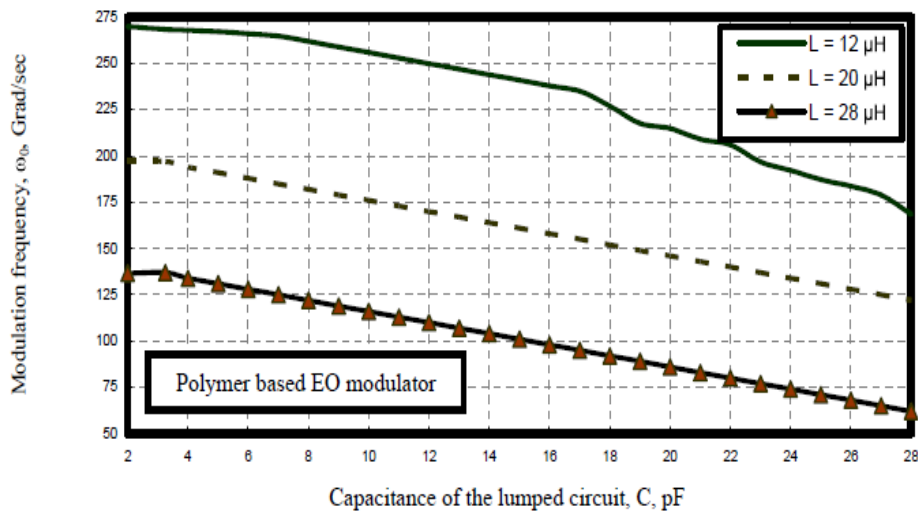


Fig. 17. Variations of modulation frequency versus capacitance of circuit at the assumed set of parameters.

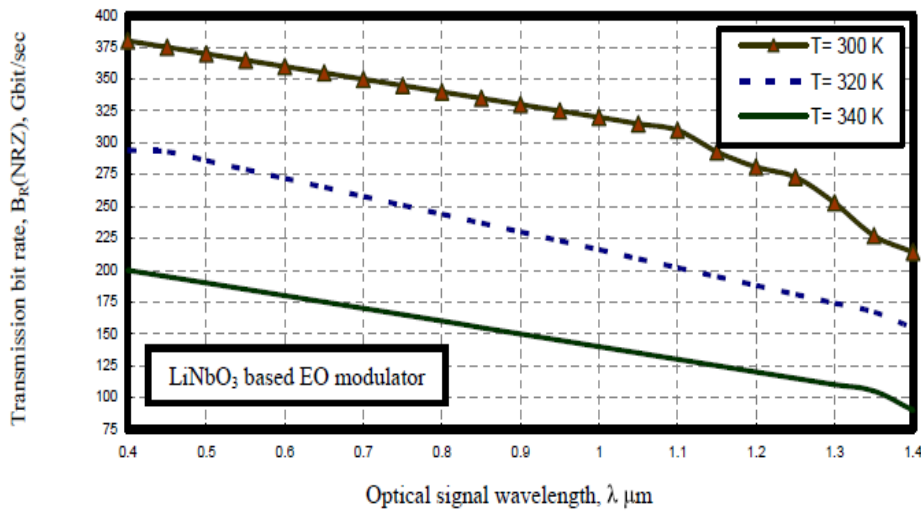


Fig. 18. Variations of transmission bit rate versus optical signal wavelength at the assumed set of parameters.

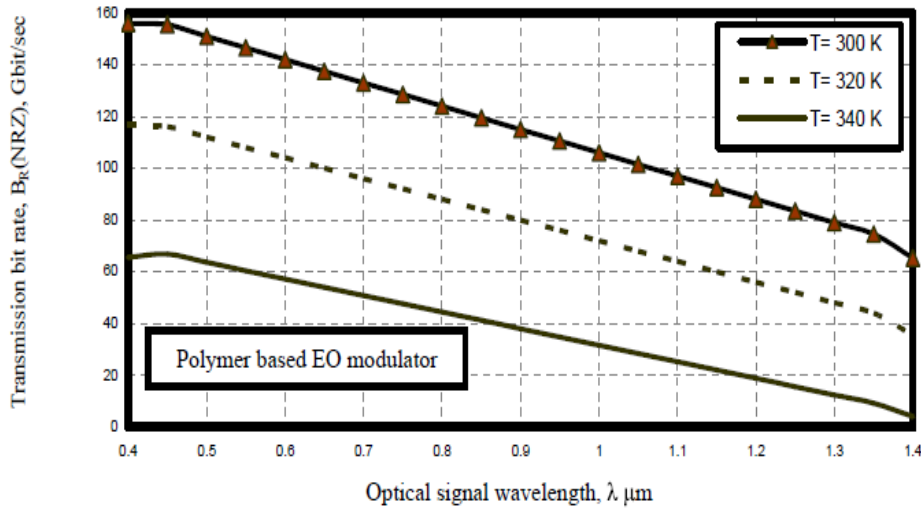


Fig. 19. Variations of transmission bit rate versus optical signal wavelength at the assumed set of parameters.

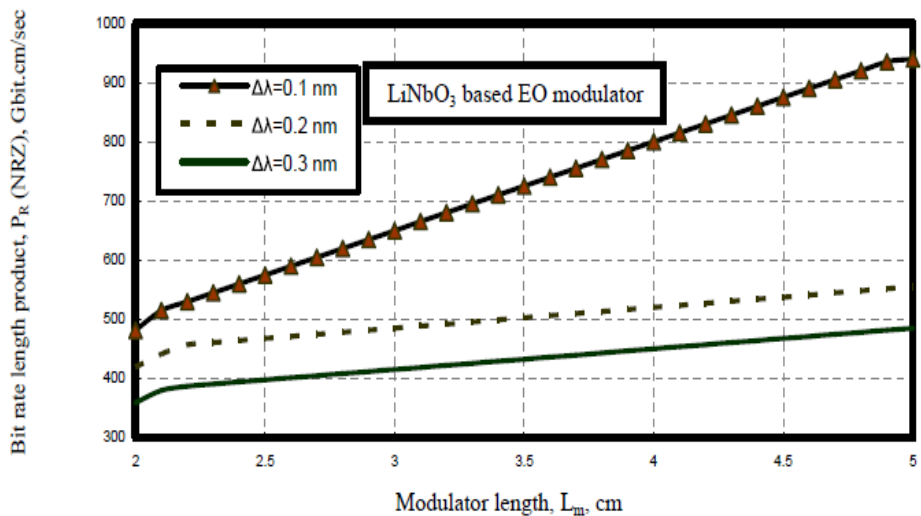


Fig. 20. Variations of transmission bit rate versus optical signal wavelength at the assumed set of parameters.

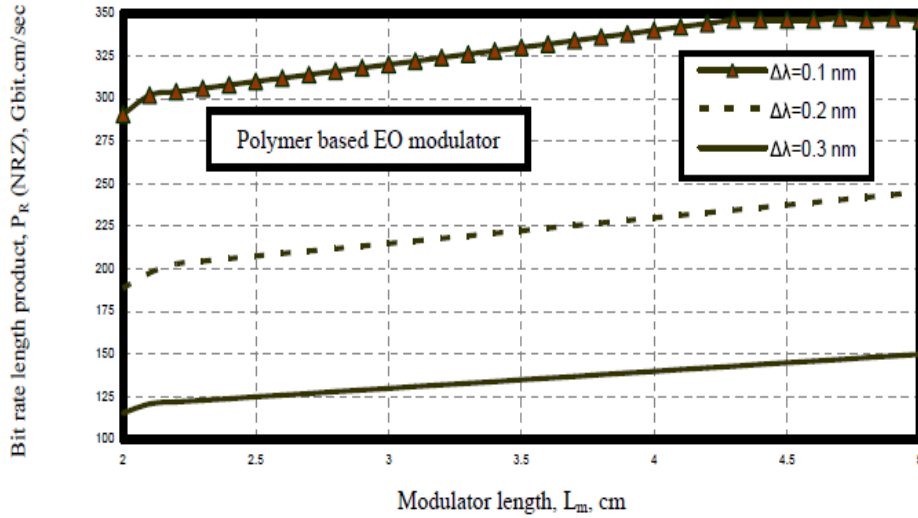


Fig. 21. Variations of transmission bit rate versus optical signal wavelength at the assumed set of parameters.

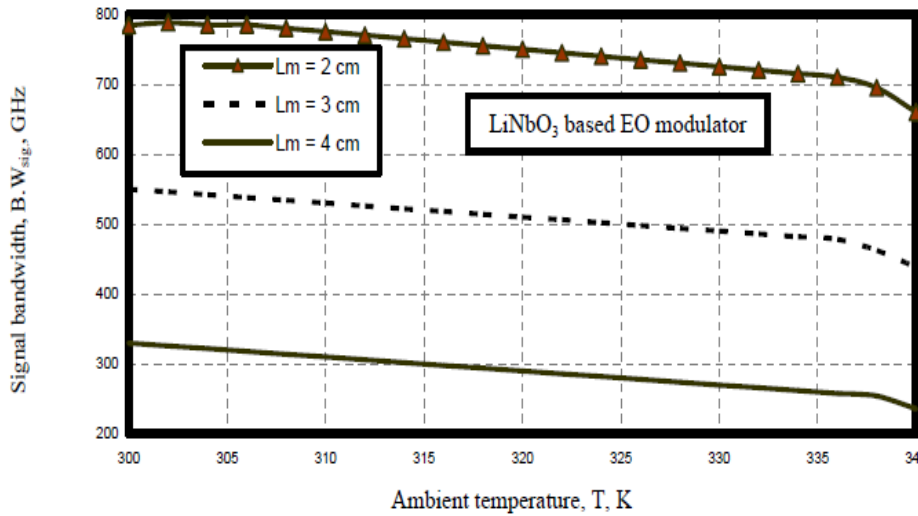


Fig. 22. Variations of signal bandwidth versus ambient temperature at the assumed set of parameters.

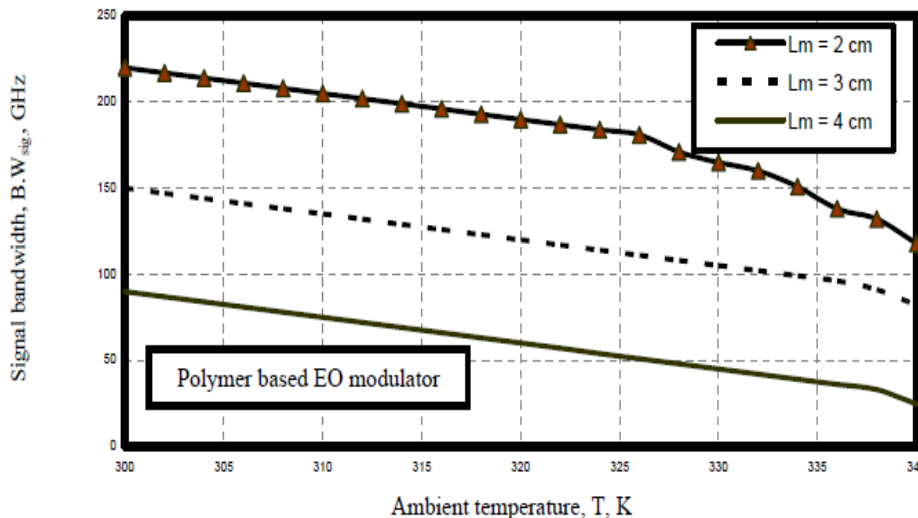


Fig. 23. Variations of signal bandwidth versus ambient temperature at the assumed set of parameters.

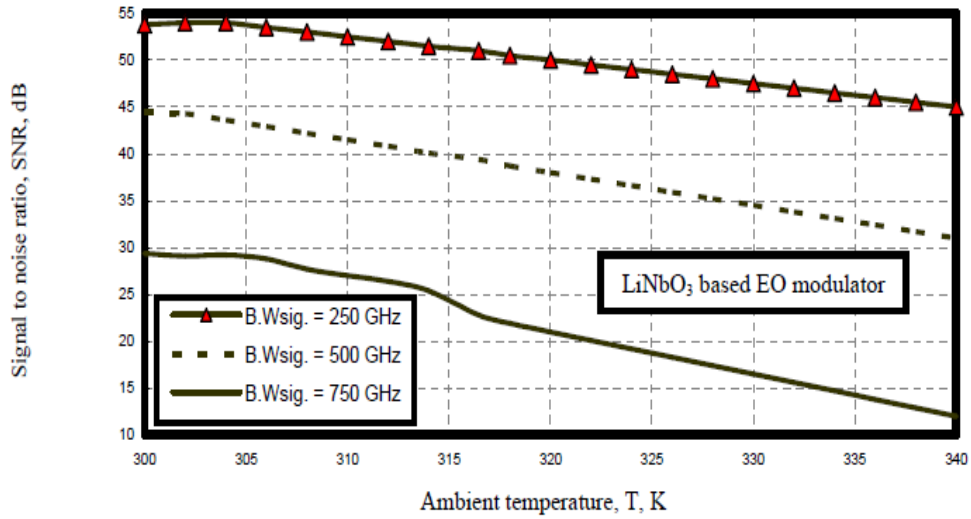


Fig. 24. Variations of signal to noise ratio versus ambient temperature at the assumed set of parameters.

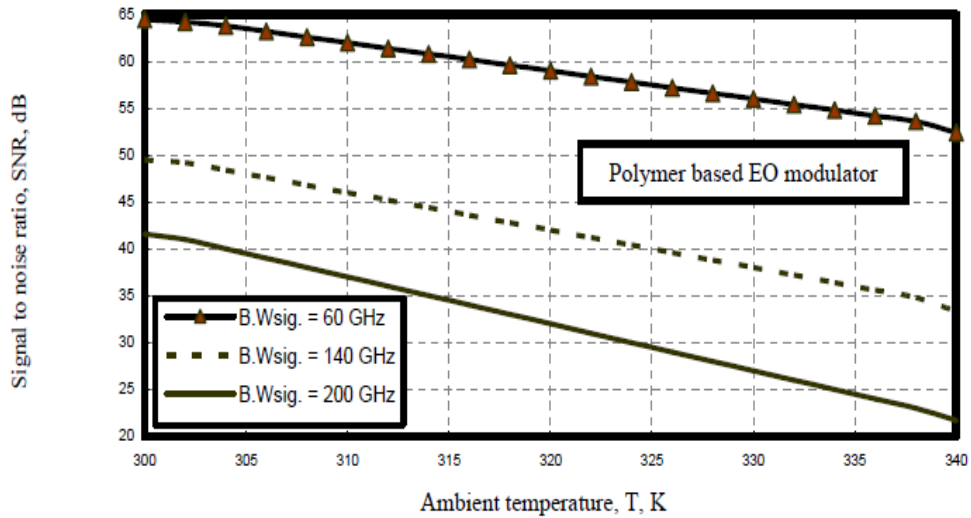


Fig. 25. Variations of signal to noise ratio versus ambient temperature at the assumed set of parameters.

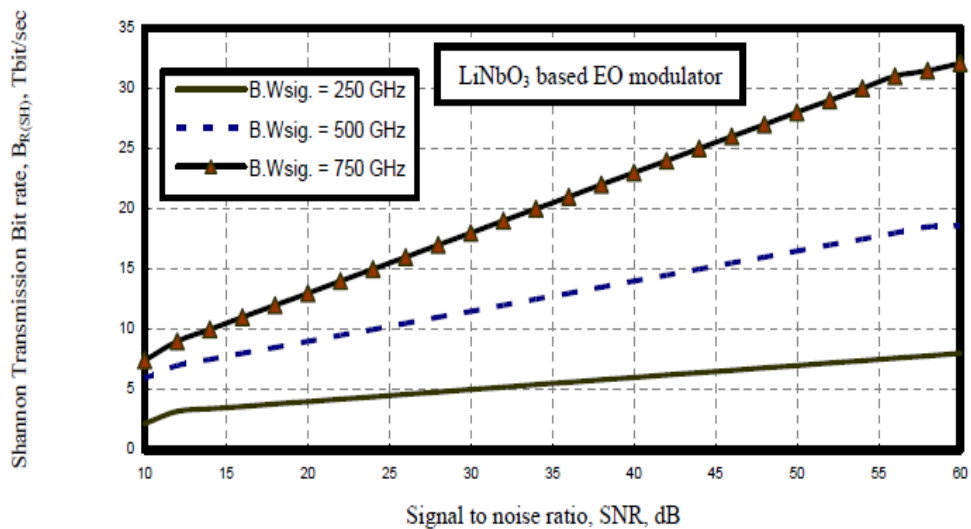


Fig. 26. Variations of transmission Shannon bit rate versus SNR at the assumed set of parameters.

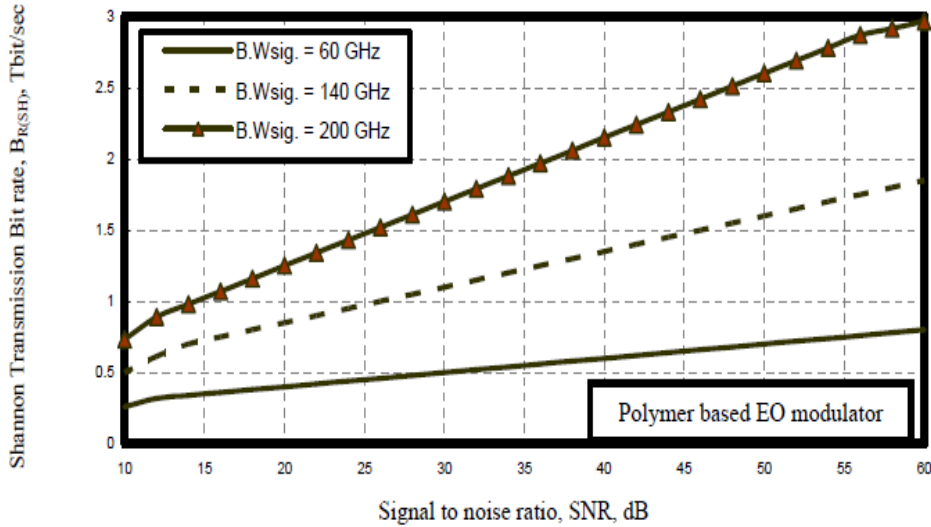


Fig. 27. Variations of transmission Shannon bit rate versus SNR at the assumed set of parameters.

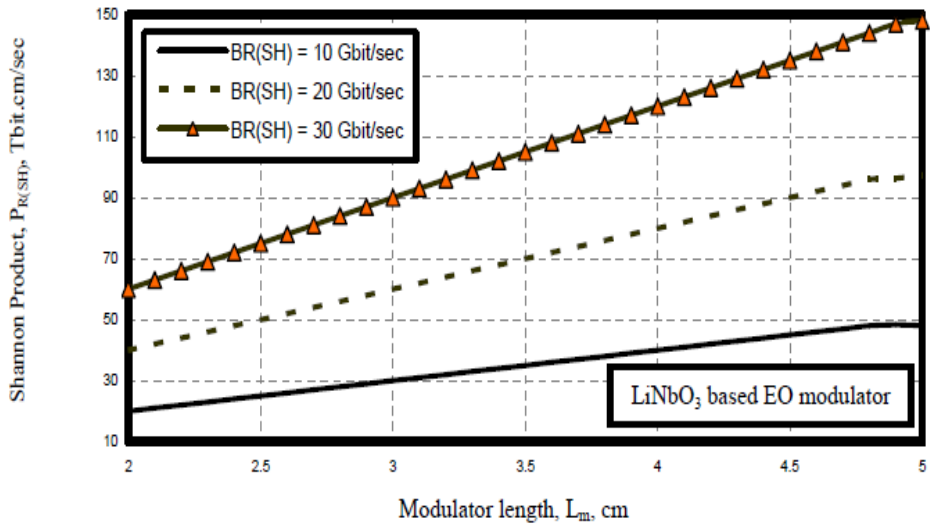


Fig. 28. Variations of transmission Shannon bit rate versus modulator length at the assumed set of parameters.

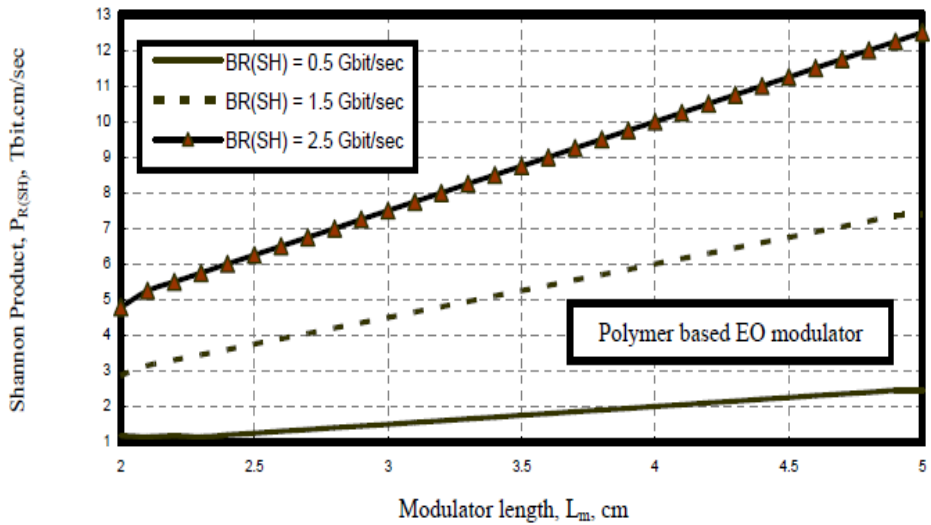


Fig. 29. Variations of transmission Shannon bit rate versus modulator length at the assumed set of parameters.

- iv) Figs. (12, 13) have proved that modulator length increases, inductance of lumped circuit decreases for both materials based EO modulator device at constant refractive index. Moreover refractive index increases for both materials based EO modulator device, inductance of lumped circuit also decreases at constant modulator length.
- v) As shown in Figs. (14, 15), as capacitance of lumped circuit for both materials based EO modulator device increases, the 3-dB modulation bandwidth decreases at constant resistance of lumped circuit. As well as resistance of lumped circuit increases, the 3-dB modulation bandwidth decreases at constant capacitance of lumped circuit.
- vi) Figs. (16, 17), as capacitance of lumped circuit for both materials based EO modulator device increases, the modulation frequency decreases at constant inductance of lumped circuit. As well as inductance of lumped circuit increases, the modulation frequency decreases at constant capacitance of lumped circuit.
- vii) Figs. (18, 19) have demonstrated that as optical signal wavelength for both materials based EO modulator device increases, the transmission bit rates decrease with NRZ code at constant ambient temperature. Moreover as ambient temperature increases, the transmission bit rates decrease at constant optical signal wavelength.
- viii) As shown in the series of Figs. (20, 21), as modulator length increases for both materials based EO modulator device, bit rate length product also increases at constant spectral line width of the optical source. But as spectral line width of the used optical source increases, the transmission bit rate length product decreases at constant modulator length.
- ix) Figs. (22, 23) have assured that as ambient temperature increases for both materials based EO modulator device, the signal bandwidth decreases at constant modulator length. As well as modulator length increases, the signal bandwidth decreases at constant ambient temperature.
- x) Figs. (24, 25) have proved that as ambient temperature increases for both materials based EO modulator device, the signal to noise ratio decreases at constant signal bandwidth. Also as signal bandwidth increases, the signal to noise ratio decreases at constant ambient temperature.
- xi) As shown in the series of Figs. (26, 27) has assured that as signal to noise ratio increases, Shannon transmission bit rates also increases as constant signal bandwidth. As well as signal bandwidth increases, the Shannon transmission bit rate also increases at constant signal to noise ratio.
- xii) Figs. (28, 29) has demonstrated that as modulator length increases, Shannon product also increases as constant transmission bit rate. Moreover as transmission bit rate increases, the Shannon product also increases at constant modulator length.

6. Conclusions

In a summary, we have showed the high speed performance of LiNbO_3 and polymer materials based electrooptic (EO) modulator in advanced optical communication systems. We have observed the increased modulator length, the increased modulator efficiency, capacitance of lumped circuit, and the decreased inductance of the lumped circuit. As well as the increased refractive index of both materials based EO modulator, the increased modulator efficiency, capacitance of lumped circuit, and the decreased inductance of the lumped circuit.

It is evident that the decreased resistance, capacitance, and inductance of lumped circuit, the increased of both modulation frequency and 3-dB bandwidth. Moreover the decreased of optical signal wavelength, spectral line width of the used optical source and ambient temperature and the increased modulator length, the increased transmission bit rates and products within NRZ coding. The decreased of both modulator length, and ambient temperature, the increased signal bandwidth. Also in the same way, the decreased of both ambient temperature and signal bandwidth, the increased signal to noise ratio. The increased of both signal to noise ratio, and the signal bandwidth lead to the increased Shannon transmission bit rates and products.

References

- [1] H. V. Pham, and Y. Okamura, "Electrooptic Modulators with Controlled Frequency Responses by Using Nonperiodically Polarization Reversed Structure," *Journal of Advances in Optoelectronics*, Vol. 8, No. 1, pp. 1-8, 2008.
- [2] T. Kawanishi, T. Sakamoto, and M. Izutsu, "High Speed Control of Lightwave Amplitude, Phase, and Frequency by use of Electrooptic Effect," *IEEE Journal of Selected Topics in Quantum Electronics*, Vol. 13, No. 1, pp. 79-91, 2007.
- [3] H. V. Pham, H. Murata, and Y. Okamura, "Travelling Wave Electrooptic Modulators With Arbitrary Frequency Response Utilising Non Periodic Polarization Reversal," *Electronics Letters*, Vol. 43, No. 24, pp. 1379-1381, 2007.
- [4] H. Tazawa and W. H. Steier, "Analysis of Ring Resonator Based Traveling Wave Modulators," *IEEE Photon. Technol. Lett.*, Vol. 18, No. 1, pp. 211-213, 2006.
- [5] G. Xu, Z. Liu, J. Ma, B. Liu, S.-T. Ho, L. Wang, P. Zhu, T. J. Marks, J. Luo, and A. K. Jen, "Organic Electrooptic Modulator Using Transparent Conducting Oxides As Electrodes," *Opt. Expr.*, Vol. 13, No. 3, pp. 7380-7385, 2005.
- [6] S.-K. Kim, H. Zhang, D. Chang, C. Zhang, C. Wang, W. Steier, and H. Fetterman, "Electrooptic Polymer Modulators With Inverted Rib Waveguide Structures," *IEEE Trans. Microw. Theory Tech.*, Vol. 15, No. 2, pp. 218-220, Feb. 2003.
- [7] J. Witzens, T. B. Jones, and M. Hochberg, "Design of Transmission Line Driven Slot Waveguide Mach-Zehnder Interferometers and Application to Analog Optical Links," *Optics Express.*, Vol. 18, No. 16, pp. 16903-16928, Aug. 2010.
- [8] A. Rahman, and S. Haxha "Optimization of Microwave Properties for Ultrahigh Speed Etched and Unetched Lithium Niobate Electrooptic Modulators," *Journal of Lightwave Technology*, Vol. 20, No. 10, pp. 1856-1863, 2002.
- [9] H. Hu, R. Ricken, W. Sohler, and R. Wehrspohn. "Lithium Niobate Ridge Waveguides Fabricated by Wet Etching," *IEEE Photonics Technology Letters*, Vol. 19, No. 6, pp. 417-419, 2007.
- [10] M. Howerton, R. Roeller, A. Greenblatt, and R. Khähenbühl, "Fully Packaged Band LiNbO₃ Modulator with Low Drive Voltage," *IEEE Photonics Technology Letters*, Vol. 12, No. 7, pp. 792-794, 2000.
- [11] Abd El-Naser A. Mohammed, M. Metawe'e, Abd El-Fattah Saad and Mohammed Tabbour, "Recent Applications of the Electrooptic Modulators in Radio Over Fiber (ROF)," *Journal of Media and Communication Studies*, Vol. 1, No. 6, pp. 106-115, Dec. 2009.
- [12] Abd El Naser A. Mohammed, Ahmed Nabih Zaki Rashed, Gaber E. S. M. El-Abyad, and Abd-El-fattah A. Saad "Applications of Conventional and A thermal Arrayed Waveguide Grating (AWG) Module in Active and Passive Optical Networks (PONs)," *International Journal of Computer Theory and Engineering (IJCTE)*, Vol. 1, No. 3, pp. 290-298, Aug. 2009.
- [13] J. G. Nollis, *Understanding Telecommunications and Lightwave Systems*, 2nd ed. IEEE Press, 1996.
- [14] M. V. Raghavendra, P. H. Prasad, "Estimation of Optical Link Length for Multi Haul Applications," *International Journal of Engineering Science and Technology*, Vol. 2, No.6, pp. 1485-1491, 2010.
- [15] I. P. Kaminow and T. L. Koch, *Optical Fiber Telecommunications, III*, New York: Academic Press, 1997.
- [16] A. Pilipetskii, "High Transmission Capacity Undersea Long Haul Communication Systems," *J. Lightwave Technol.*, Vol. 12, No. 4, pp. 484-496, 2006.
- [17] Abd El-Naser A. Mohammed, Abd El-Fattah A. Saad, and Ahmed Nabih Zaki Rashed and Mahomud M. Eid, "Characteristics of Multi-Pumped Raman Amplifiers in Dense Wavelength Division Multiplexing (DWDM)

Optical Access Networks,” IJCSNS International Journal of Computer Science and Network Security, Vol. 9, No. 2, pp. 277-284, Feb. 2009.

- [18] Abd El-Naser A. Mohammed, and Ahmed Nabih Zaki Rashed, “Comparison Performance Evolution of Different Transmission Techniques With Bi-directional Distributed Raman Gain Amplification Technique in High Capacity Optical Networks,” International Journal of Physical Sciences, Vol. 5, No. 5, pp. 484-495, May 2010.

Author



Dr. Ahmed Nabih Zaki Rashed was born in Menouf city, Menoufia State, Egypt country in 23 July, 1976. Received the B.Sc., M.Sc., and Ph.D. scientific degrees in the Electronics and Electrical Communications Engineering Department from Faculty of Electronic Engineering, Menoufia University in 1999, 2005, and 2010 respectively. Currently, his job carrier is a scientific lecturer in Electronics and Electrical Communications Engineering Department, Faculty of Electronic Engineering, Menoufia university, Menouf. Postal Menouf city code: 32951, EGYPT. His scientific master science thesis has focused on polymer fibers in optical access communication systems. Moreover his scientific Ph. D. thesis has focused on recent applications in linear or nonlinear passive or active in optical networks.

His interesting research mainly focuses on transmission capacity, a data rate product and long transmission distances of passive and active optical communication networks, wireless communication, radio over fiber communication systems, and optical network security and network management. He has published many high scientific research papers in high quality and technical international journals in the field of advanced communication systems, optoelectronic devices, and passive optical access communication networks. His areas of interest and experience in optical communication systems, advanced optical communication networks, wireless optical access networks, analog communication systems, optical filters and Sensors, digital communication systems, optoelectronics devices, and advanced material science, network management systems, multimedia data base, network security, encryption and optical access computing systems. As well as he is editorial board member in high academic scientific International research Journals. Moreover he is a reviewer member in high impact scientific research international journals in the field of electronics, electrical communication systems, optoelectronics, information technology and advanced optical communication systems and networks. His personal electronic mail ID (E-mail:ahmed_733@yahoo.com).

